

Energy-dissipative Semi-Active Tuned Mass Damper Building Systems for Structural Damage Reduction

Min-Ho Chey¹, J. Geoffrey Chase², John B. Mander³ and Athol J. Carr⁴

¹Department of Architecture and Art, Yanbian University of Science and Technology, Yanji City, Jilin, China

²Department of Mechanical Engineering, University of Canterbury, Christchurch, New Zealand

³Zachry Department of Civil Engineering, Texas A&M University, TX 77843-3136, USA

⁴Department of Civil and Natural Resources Engineering, University of Canterbury, Christchurch, New Zealand

I. Abstract

Realistic 12-story energy-dissipative Tuned Mass Damper (TMD) building systems are proposed to mitigate story and structural damage due to seismic loads. The upper two and four stories are isolated and used as the tuned mass, saving excessive non-functional added weight. Further, it is proposed to replace the passive spring damper with semi-active resettable devices, creating more adaptive resettable device based semi-active TMD (SATMD) systems. Semi-actively manipulating the reaction forces effectively retunes the system depending on the structural response, offering a broader more adaptive solution than passive tuning. This proposal thus combines emerging semi-active devices with existing tuned mass damper concepts to create extended seismic response mitigation applications. Inelastic time history analyses are used to demonstrate the efficacy of this concept. Performance is measured in terms of dissipated hysteretic energy and weighted damage values. The SATMD systems outperform passive solutions in most cases, by at least 10%, especially if the passive tuning is not optimal or exact. The impact on the mode shapes and modal contributions is also markedly different for the systems, further illustrating the differences in performance obtained.

Key words: tuned mass damper, seismic isolation, semi-active control, resettable device, seismic hazard

II. Introduction

TMD systems are one of the practical, well accepted strategies in the area of structural control for flexible structures. Particularly for tall buildings that are not amendable to base isolation or other approaches. They consist of added mass with properly tuned spring and damping elements, providing a frequency-dependent hysteresis that increases damping in the primary structure. The mechanism of suppressing structural vibrations by attaching a TMD to the structure is to transfer the vibration energy of the structure to the TMD and to dissipate the energy in the damper of the TMD. A number of TMDs have been installed in tall buildings, bridges, towers, and smoke stacks for response control (Kawabata et al. 1990; Khan 1983; Kwok and Macdonald 1990; McNamara 1977; Ueda et al. 1993). Hence, this passive seismic mitigation approach can be considered to be very well accepted.

This passive TMD (PTMD) approach is undoubtedly a simple, inexpensive and somewhat reliable means to suppress the undesired vibrations. However, one of the limitations to the TMD design is the narrow bandwidth of the frequency tuned control it provides. The resulting potential fluctuation or error in tuning of the TMD frequency to the controlled frequency of a structure means that the PTMD is not entirely reliable or robust in all cases despite its passive nature. Furthermore, the method used to support the large added mass and provide precise frequency control is an important issue in the design of a TMD and can introduce error in the tuning.

Thus, the ultimate performance of the TMD system is limited by the size of the additional mass, where is typically 0.25~1.0% of the building's weight in the fundamental mode, as well as the potential for tuning error or non-optimal implementation. In the latter case, even small tuning errors due to structural frequency degradation over time can result in significant reductions in performance.

In an attempt to increase the performance of the TMD without incurring the sensitivity related tuning problem, active TMD (ATMD) systems have been proposed (Abdel-Rohman 1984; Chang and Yang 1995; Chang and Soong 1980; Li et al. 2003). It has been reported that ATMD can provide better suppression of structural vibrations than PTMD systems. However, ATMDs have the disadvantages of added complexity, high operational and maintenance costs, and high power requirements. Hence, they are considered less reliable than passive systems, limiting implementation to special certain cases.

III. Modified TMD systems and semi-active control strategy

To overcome limitations on the mass of the TMD, it has been suggested that using a portion of the building itself as a tuned mass may be more effective. Thus, the seismic isolation concept using TMD design principles has been extended to convert a structural system. In particular, one idea is to use the building's upper mass as the tuned mass. Recognizing the potential design and performance benefits, as well as the limitations of ATMD systems, a new class of semi-active tuned mass damper (SATMD) has been introduced. Semi-active control systems are a distinctly and emerging class of active control systems. Typically, semi-active control devices do not add mechanical energy to the structural system (including the structure and the control actuators) avoiding the large power requirements of ATMDs. In addition, its adaptive response to structural response sensor feedback provides the wide bandwidth of control, unlike narrowly tuned PTMDs, but very similar to ATMDs. Hence, the combined concept of modified TMD system and semi-active control strategy provides an extremely promising alternative to PTMD and ATMD designs.

1) Top story and roof isolation systems

The concept of an 'expendable top storey' (Jagadish et al. 1979), or the 'energy absorbing storey' (Miyama 1992), is an effective alternative where the top story acts as a vibration absorber for the lower stories. Villaverde et al. (2002) studied a 13-story building to assess the viability and effectiveness of a 'roof isolation' system aimed at reducing the response of buildings to earthquakes. Hence, the proposal to build a vibration absorber with a building's roof or upper stories has the potential to become an attractive way to reduce structural and nonstructural earthquake damage in low- and medium-rise buildings as well as a mean of avoiding excessive added mass for a typical TMD design.

2) Mid-story isolation systems

Some researchers (Charng 1998; Pan et al. 1995; Pan and Cui 1998) sought to evaluate the effect of using segmental structures, where isolation devices are placed at various heights in the structure and at the base to reduce displacements. Each segment may comprise a few stories and is interconnected by additional vibration isolation systems. Charng (1998) suggested three possible design methods to link two segments to prevent the occurrence of rocking modes and transmit gravity loads between the two segments. Murakami et al. (2000) described the design of a multifunctional 14-story building accommodating apartments, office rooms and shops, where a seismic isolation system is installed on the middle story.

3) Semi-active TMD systems

Hrovat et al. (1983) used semi-active TMDs with variable damping components for the control of wind-induced vibrations in tall buildings. Abe (1996) studied a variation of semi-active TMDs with pulse generators for the seismic protection of civil structures. Pinkaew and Fujino (2001) presented a SATMD with

variable damping under harmonic excitation and showed that the semi-active optimal control becomes a clipped optimal control law. The effectiveness of a semi-active variable stiffness tuned mass damper (SAIS-TMD) in response control of 76-story tall buildings was studied and its performance was evaluated analytically (Varadarajan and Nagarajaiah 2004). Finally, Mulligan et al. (Mulligan et al. 2006; Mulligan 2007) investigated spectral analyses and the design of SATMD systems for suites of probabilistically scaled events accounting for the impact of ground motion on response and performance.

IV. Semi-active resettable device

1) Conventional resettable devices

The originally proposed resettable device (Jabbari and Bobrow 2002) has both chambers connected via a valve that can be internal or external to the device as depicted in Fig. 1. This valve controls the hysteretic response of the device by holding or releasing the pressure between the chambers. The valve is activated, equilibrating the pressure in each chamber, on the peak displacement in each cycle resulting in a dissipative force-displacement hysteretic loop.

However, this original design configuration limits the hysteretic response shape that can be obtained and, in larger devices, its full force potential. More specifically, the chambers are directly linked so that the pressure in each chamber is a function of the pressure in the other chamber. This interdependency affects the energy release time, as large devices with high pressure and larger chamber volumes require more time for the active chamber to revert or return to equilibrium pressure on resetting. This time period can be significant compared to structural response periods (Chase et al. 2006). As a result, while the chambers equilibrate the active chamber cannot be utilized to resist motion by compressing the working fluid, thus significantly affecting performance.

2) Resettable devices with independent chambers

To overcome the limitations involved with energy release time and the limited hysteretic response of the single valve design, a device with a valve on each chamber was designed, as illustrated in Fig. 2. Using this novel independent chamber design, the pressure in each chamber is no longer a function of the pressure in the other chamber. In addition, the resetting of each chamber does not require the other chamber to be reset or effectively out of use at the same time. Thus, hysteretic behaviors that are not possible with the single valve design become apparent.

Most importantly, by independently controlling each chamber, the energy reset time is able to be much longer, as motion can be resisted by the other chamber during this time. Hence, this design controls the pressure-volume state of each chamber independently. As a result, the active chamber can be utilized to resist motion effectively instantly without waiting for the energy release to be completed for the other chamber. Equally importantly, independent control of each chamber allows a far wider range of device force-displacement behavior.

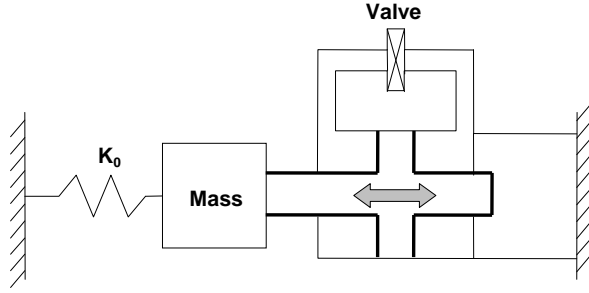


Fig. 1. Schematic of a single-valve resettable device attached to a single-degree-of-freedom system.

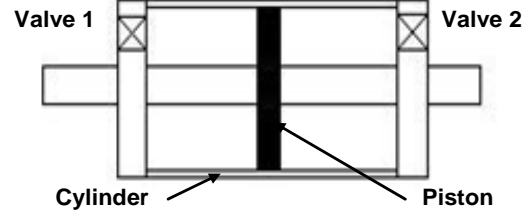


Fig. 2. Schematic of independent chamber design

V. SATMD building system

1) Introduction

The proposed TMD building system concept can be defined as an extension of the conventional TMD system, but using relatively much larger mass ratio. Due to the large mass ratio, the upper portion may experience large displacement. To avoid excessive lateral motion or stroke of the tuned mass, the upper portion can be interconnected by a combined isolation system of rubber bearings and a viscous damper (for the PTMD passive version) or resettable devices (for the resettable SATMD proposed here). When the building frame is implemented with the proposed TMD (PTMD or SATMD) system, the upper portion is supported by rubber bearings attached on the top of the main frame's columns to support gravity loads.

2) Motion characteristics and equations

For the TMD (PTMD or SATMD) building systems, a 2-DOF system can be defined for design by a pair of coupled second-order ordinary differential equations. These simple systems can be used for design analysis before detailed non-linear analysis of any specific case study. For the PTMD and SATMD building systems, the equations of motion of the systems subjected to the earthquake load can be defined respectively:

$$\begin{bmatrix} m_1 & 0 \\ 0 & m_2 \end{bmatrix} \begin{Bmatrix} \ddot{x}_1 \\ \ddot{x}_2 \end{Bmatrix} + \begin{bmatrix} c_1 + c_2 & -c_2 \\ -c_2 & c_2 \end{bmatrix} \begin{Bmatrix} \dot{x}_1 \\ \dot{x}_2 \end{Bmatrix} + \begin{bmatrix} k_1 + k_2 & -k_2 \\ -k_2 & k_2 \end{bmatrix} \begin{Bmatrix} x_1 \\ x_2 \end{Bmatrix} = \begin{Bmatrix} k_1 \\ 0 \end{Bmatrix} x_g + \begin{Bmatrix} c_1 \\ 0 \end{Bmatrix} \dot{x}_g \quad (1)$$

$$\begin{bmatrix} m_1 & 0 \\ 0 & m_2 \end{bmatrix} \begin{Bmatrix} \ddot{x}_1 \\ \ddot{x}_2 \end{Bmatrix} + \begin{bmatrix} c_1 & 0 \\ 0 & 0 \end{bmatrix} \begin{Bmatrix} \dot{x}_1 \\ \dot{x}_2 \end{Bmatrix} + \begin{bmatrix} k_1 + k_{2(RB)} + k_{2(res)} & -k_{2(res)} & k_{2(res)} \\ -k_{2(RB)} - k_{2(res)} & k_{2(RB)} & k_{2(res)} \end{bmatrix} \begin{Bmatrix} x_1 \\ x_2 \\ x_s \end{Bmatrix} = \begin{Bmatrix} k_1 \\ 0 \end{Bmatrix} x_g + \begin{Bmatrix} c_1 \\ 0 \end{Bmatrix} \dot{x}_g \quad (2)$$

where m_1 = mass of main system; m_2 = mass of TMD; k_1 = stiffness of main system; $k_{2(RB)}$ = stiffness of rubber bearings; $k_{2(res)}$ = stiffness of resettable device; c_1 = damping coefficient of main system; c_2 = damping coefficient of TMD; x_1 = displacement of main system; x_2 = displacement of TMD; x_g = displacement of ground; and x_s = equilibrium position (unstretched length) of the resettable spring from its last reset point.

The resettable device stiffness, and thus force, $k_{2(res)}$, is modeled as a variable stiffness spring element based on the relative motion between the lower mass and the isolated upper mass. Note that a resettable device non-linearly alters the stiffness as a function of its motion, creating a non-linear dynamic system with (implicit) feedback control, in contrast to the linear PTMD system model.

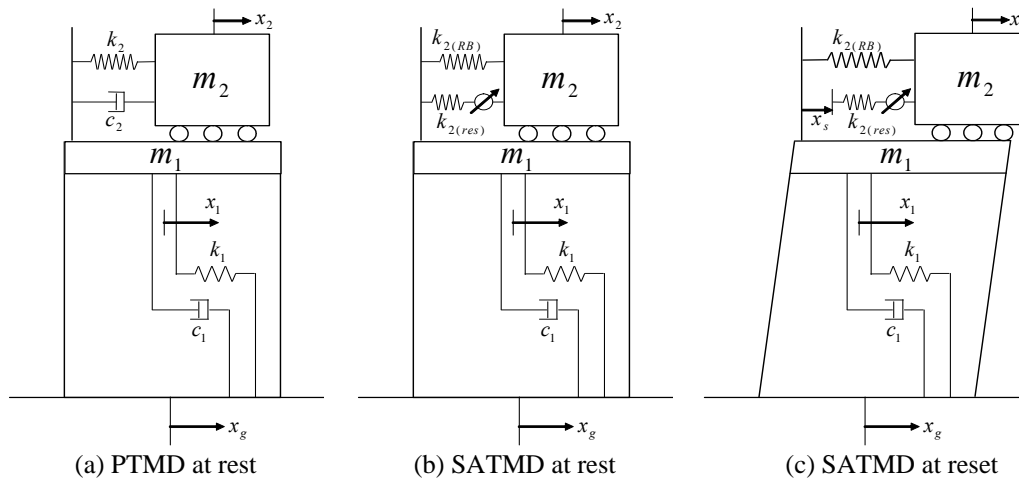


Fig. 3. TMD building system models for 2-DOF design analyses

VI. 12-story SATMD building system

1) Structural configuration

A 12-story, two-bay reinforced concrete framed structure is used to demonstrate the potential and beneficial effects of TMD building systems (Jury 1978). This model was designed originally according to the New Zealand Loadings Code (NZS4203 1976) based on the concept of capacity design. For SATMD and PTMD systems, the upper two and four stories are isolated. The resulting retrofitted structures are thus modeled as ‘10+2’ story and ‘8+4’ story structures, as shown in Fig. 4. Hence, two cases are presented for 12-story SATMD/PTMD building systems, which differ by the mass ratio used as a function of extra stories.

The member sizes adopted in this study are shown in Table 1. The dynamic properties of the uncontrolled 8-story and 10-story frames under the isolation layer, such as the natural frequency, modal effective mass, modal damping ratios, and participation factors, are calculated and listed in Table 2. Fig. 5 shows the schematic description of isolation layer including rubber bearings and viscous damper or resettable device.

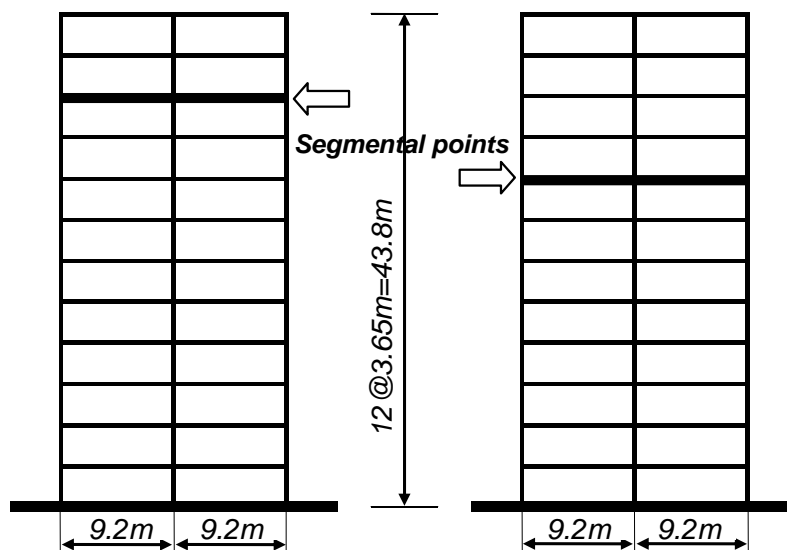


Fig. 4. ‘10+2’ and ‘8+4’ models of 12-story two-bay reinforced concrete frames

Table 1. Member sizes of the frame

Members	Level	Dimensions(mm)
Beams	1 – 6	900 × 400
	7 – 8	850 × 400
	9 – 12	800 × 400
Exterior Columns	1 – 6	775 × 500
	7 – 8	750 × 500
	9 – 12	650 × 500
Interior Column	1 – 6	800 × 800
	7 – 8	725 × 725
	9 – 12	675 × 675

Table 2. Dynamic properties of the frame structures

Item	8-story	10-story	Unit
Weight	12,940	16,080	kN
1 st Modal Mass	1,072	1,301	ton
Natural period	1.187	1.518	sec
Frequency	5.30	4.14	rad/sec
Damping Ratio	0.05	0.05	-
1 st Modal Amplitude	1.309	1.343	-

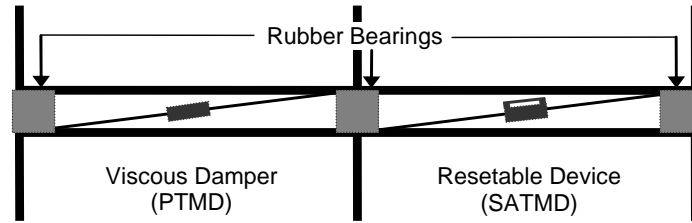


Fig. 5. Schematic description of isolation layer

2) TMD Optimization

For the optimum TMD parameters, it was found that the tuning ratio for a MDOF system is nearly equal to the tuning ratio for a 2-DOF system for a mass ratio of $\mu\Phi$, where Φ is the amplitude of the first mode of vibration for a unit modal participation factor computed at the location of the TMD (Sadek et al. 1997). Thus, the equation for the tuning and damping ratios are obtained from the equation for the 2-DOF system by replacing μ by $\mu\Phi$, yielding:

$$f_{M2opt} = \frac{1}{1 + \mu\Phi} \left(1 - \xi_1 \sqrt{\frac{\mu\Phi}{1 + \mu\Phi}} \right) \quad \xi_{M2opt} = \Phi \left(\frac{\xi_1}{1 + \mu} + \sqrt{\frac{\mu}{1 + \mu}} \right) \quad (4)$$

The practical parameters of the optimal TMD stiffness and the optimal damping coefficient can be thus derived:

$$k_{M2opt} = m_2 \omega_1^2 f_{M2opt}^2 = \frac{m_2 \omega_1^2}{(1 + \mu\Phi)^2} \left(1 - \xi_1 \sqrt{\frac{\mu\Phi}{1 + \mu\Phi}} \right)^2 \quad (5)$$

$$c_{M2opt} = 2m_2 \omega_1 f_{M2opt} \xi_{M2opt} = \frac{2m_2 \omega_1}{1 + \mu\Phi} \left(1 - \xi_1 \sqrt{\frac{\mu\Phi}{1 + \mu\Phi}} \right) \left(\frac{\xi_1}{1 + \mu} + \sqrt{\frac{\mu}{1 + \mu}} \right) \quad (6)$$

The resulting optimum parameters are listed in Table 3. The total value of k_{M2opt} is allocated to rubber bearing stiffness and the stiffness of the SA resetable device. According the results from the 2-DOF analysis for the system design (Chey et al. 2007), the SATMD having same stiffness values of the resetable device and the rubber bearings has been chosen and adopted for each structure and earthquake suite. This equivalent combined

stiffness was chosen for simplicity and may not represent an optimal SATMD design (Mulligan 2006), where much lower stiffness values may be used. Note that the values of ζ_{M2opt} are very large, representing of optimal, but not necessarily feasible, implementation solution. In this analysis, these values are used to present the most difficult comparison for the SATMD alternative.

Table 3. Parameters for the TMD building systems studied.

Model	μ	f_{M2opt}	ζ_{M2opt}	k_{M2opt} (kN/m)	c_{M2opt} (kN-s/m)	Device Force (kN)
PTMD(10+2)	0.244	0.734	0.649	2,935	1,252	-
SATMD(10+2)	0.244	0.734	-	2,935	-	644
PTMD(8+4)	0.594	0.544	0.840	5,293	3,085	-
SATMD(8+4)	0.594	0.544	-	5,293	-	1,573

3) Modal analysis

Modal analysis results using Ruaumoko are shown in Fig. 6. The TMD building systems now offer two major modes of vibration instead of one in the 12-story uncontrolled (No TMD) case. Despite having two major modes and thus a system susceptible to receiving larger amounts of input energy from an earthquake, a relatively large portion of the entrapped energy is concentrated in the isolation layer. For the SATMD building systems, the 1st mode dominates the upper stories and a much smaller magnitude 2nd mode dominates the lower story response. Thus, both the 1st and 2nd modes of the original structure are decoupled by the isolation layer.

These results indicate two different methods of dissipating energy. The PTMD dissipates energy via tuned absorption. However, the SATMD dissipates energy via enhanced relative motion obtained by decoupling the structural segments. The modal participation factor for the *i*th mode is defined as:

$$\Gamma_i = \frac{L_i}{M_i} \tag{7}$$

where L_i is the earthquake excitation factor for the *i*th mode, and M_i is the generated modal mass of that mode. Another useful parameter for the modal response analysis is the mass participation factor.

$$\beta_i = \frac{M_{eff,i}}{M} = \frac{1}{M} \frac{L_i^2}{M_i} \tag{8}$$

where $M_{eff,i}$ is the effective mass for the *i*th mode and M is the total mass of the building. Because the effective mass indicates the importance of the contribution of the *i*th mode to the total base shear acting on the structure, the mass participation factor can be an index showing how much of the total mass of the building will contribute in generating base shear in that mode. Thus, if the mass participation factor of the 1st mode is much higher than that of the 2nd mode, the 1st mode can be readily excited by base excitation.

Table 4 shows the numerical results of this modal analysis. Second modal participation factors of the SATMD (10+2 and 8+4) building systems are closer to those of the first mode and relatively larger than those of the second mode for the PTMD system. Furthermore, the second mass participation factors of the SATMD building systems are larger than those of the first modes. Therefore, in the SATMD building system, the interaction between the first and second modes is more pronounced and the relatively larger mode and mass

participations of the second mode for the SATMD building system may contribute to the further reduction of the overall responses of displacement and base shear responses compared to the PTMD results.

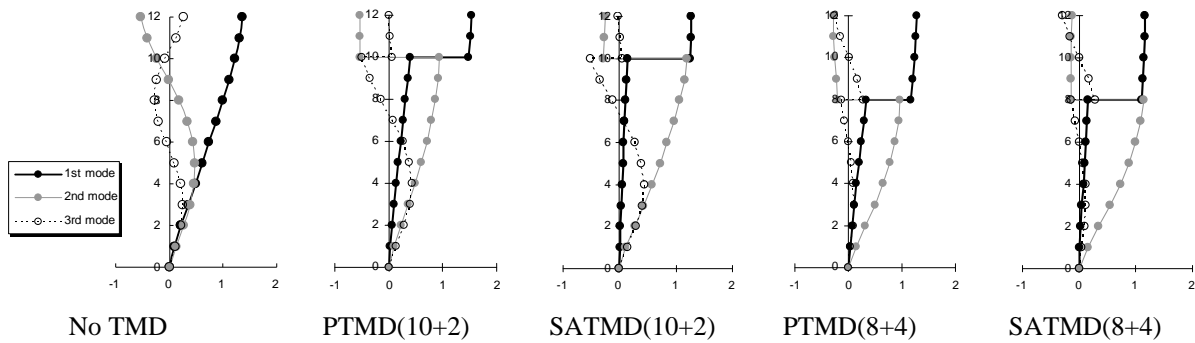


Fig. 6. Mode shapes of ‘10+2’ and ‘8+4’ models (PTMD and SATMD)

Table 4. Numerical results of modal analysis

TMD	Mode	Mass (kN·s ² /m)	Frequency (rad/sec)	Participation Fact.	
				mode	mass
No TMD	1 st	1514	0.53	1.37	0.805
	2 nd	252	1.52	-0.53	0.134
	3 rd	74	2.73	-0.27	0.039
PTMD (10+2)	1 st	816	0.38	1.53	0.436
	2 nd	812	0.74	0.94	0.434
	3 rd	181	1.92	-0.50	0.097
SATMD (10+2)	1 st	513	0.27	1.27	0.274
	2 nd	1109	0.68	1.20	0.593
	3 rd	187	1.90	-0.50	0.100
PTMD (8+4)	1 st	1020	0.36	1.29	0.541
	2 nd	697	0.96	0.97	0.370
	3 rd	39	2.39	0.28	0.021
SATMD (8+4)	1 st	834	0.27	1.17	0.442
	2 nd	878	0.89	1.15	0.465
	3 rd	47	2.33	-0.30	0.025

4) Nonlinear effects and performance indices

The assessment of the input energy represents a good starting point to develop a seismic design method based on energy criteria. However, even though the input energy demand can be considered a good indicator of the damage potential of the earthquake (Bertero and Uang 1992; Conte et al. 1990), it must be noted that only a small percentage of the input energy is dissipated, as hysteretic energy related to seismic structural damage.

Damage analyses were carried out for the prototype structures using the results obtained from nonlinear time history analyses. The Park & Ang (1985) structural damage index was used in evaluating overall structural damage when the structural displacement ductility is near the design structural ductility. Furthermore, attention is focused on overall structural damage indices because these parameters summarily lump all existing damage in members in a single value that can be easily correlated to single-value seismic parameters. For this

purpose, the programme, Ruaumoko uses a modified damage index. In this slightly modified damage model, the global damage is obtained as a weighted average of the local damage at the ends of each element, with the dissipated energy as the weighting function.

To demonstrate the accurate and valid controlled performances of the SATMD building systems, inelastic time history analyses are used. These analyses are based on nonlinear structural models including nonlinear P-delta effects and a modified Takeda hysteresis model. In addition, interstory drift ratio, dissipated hysteretic energy and weighted damage values are also evaluated as performance indices.

VII. Earthquake suites and statistical analysis methodology

As the characteristics of seismic excitation are entirely random and vary significantly, the use of a number of multiple time history records over a range of seismic levels is essential for effective controller evaluation. The three ground motion acceleration suites used here were developed by Sommerville et al. (1997) for the SAC Phase II project. Each suite has, 10 pairs of recorded or generated ground motion accelerograms selected to fit the magnitude and distance characteristics of the seismic hazard at the LA site

The first suite represents ground motions for which the structural demand has a 50% chance of being exceeded in 50 years (Low suite). The second suite represents a 10% chance in 50 years (Medium suite) and the final (High) suite a 2% chance in 50 years. To reduce the computational requirements, the first of each of the 10 pairs of records (odd half) are used in this paper.

To combine these results across the earthquakes in a suite, log-normal statistics are used (Hunt 2002; Limpert et al. 2001). For the statistical assessments, the response measures are each defined with respect to a single seismic event. These results can then yield (using log-normal statistics) a 50th percentile value and 1-2 multiplicative standard deviations. In this paper the first such standard deviation covers the 16th-84th percentile responses at that probability level, providing a measure of the robustness of the design over the suite.

To present a summary of the distribution change between the controlled (PTMD and STMD) and uncontrolled (No TMD) data sets, while providing accurate statistical measures that are not highly affected by changes in any single variable, 50th percentile and 84th percentile are presented. It should be noted that the structural hysteretic energy does not follow a lognormal distribution, unlike peak drift and peak acceleration (Breneman 2000). To define a statistical measure of the energy dissipation response values, the standard “counted” mean and 84th percentile are therefore used for this metric.

VIII. Seismic performances

1) Interstory drift ratio

Fig. 7 and 8 show the maximum interstory drift ratios resulting from the analyses. For the low suite, the 50th percentile drifts of the No TMD system are reasonably uniform over the height of the structure and the peak drift occurs in the 9th story. However, the TMD systems reduced the response of the isolated upper stories, as well as the lower stories. The profiles clearly reflect the systematic advantage of the SATMD systems. Though increasing the level of seismic hazard increases the interstory drift, the increased ratios of the drift in the isolated upper stories are still small and again the peak drift locations are shifted to the lower stories. For the low and medium sets of motion, all the drift demands of the TMD systems are less than the life safety limit of 2.5% for the numerical time history analysis specified in NZS4203 (1992).

2) Story and structural hysteretic energy

The hysteretic energy dissipated by the frame members at each floor along the height of the structures are developed in Fig. 9 and 10. As expected, from increasing story drift demands, as the severity of ground motions increases the amount of hysteretic energy dissipated by the structure members increases. The comparison of these figures shows that the higher level of hazard produces high energy demands in the lower stories and the energy distribution patterns correspond to the drift demands of the structure.

In particular, clearly lower energy demands at upper stories which are above the isolation layer can be found due to its interception of the energy flow up from the base. This structural property produces the reduced energy demands of the lower stories too. In other words, the amount of transferred energies from the base was decreased by splitting the lump of overall structural mass and, therefore, the dissipated energy along the height is reduced. In the low suite of motions, the energy curves of the isolated upper structures lie along the y-axis, as they are successful in isolating and maintaining the upper structure within the limits of elastic behavior. In the medium and high suite responses, the TMD systems are still successful at keeping the response essentially linear, as indicated by very low values of hysteretic energy indices.

Finally, as a representative energy value, all of the dissipated energy values along the height are summed to establish a total structural hysteretic dissipated energy index, as seen in Fig. 11 and 12. Again, the control effects are shown to become significant for the larger mass ratio (8+4) and the SATMD system, and the control effectiveness difference is pronounced from the PTMD(10+2) to the SATMD(8+4) systems. Overall, all the TMD systems were successful in reducing the seismic hysteretic energy demands at all hazard levels.

3) Story and structural damage

The distribution of story damage indices are shown in Fig. 13 and 14. Story damage indices are based on the member damage indices in a level. It can be said that the distribution of story damage has a similar pattern to that of story dissipated energy, which is used as a weighting factor for the calculation of the damage index. The only difference between these two indices is from the part of structural deformation. It can be seen that all of the TMD systems suffer insignificant repairable story damage up to the 50th percentile of the medium suite. Only the 1st level of the TMD systems suffers significant damage for the 84th percentile of the high suite, which gives damage indices over 1.0. The figures also show that the damage indices of the upper isolated stories for every suite are less than 0.4 at each level, which indicates, again, the effective interception of energy flow at the isolation layer. Overall, it seems that the main benefits of the reduced damage demands are on the upper stories for each suite, rather than for the lower stories.

The structural damage indices, which indicate the damage of the whole structure, are summarized in Fig. 15 and 16. The structural damage indices are obtained as a weighted average of the local damage at the ends of each element, with the dissipated energy as the weighting function. The structural damage indices for all suites are less than 0.4 except for the 84th percentile of the high suite. Hence, all of the TMD systems are repairable for those suites. Even for the 84th percentile of the high suite, the structural damage indices are under 1.0, which indicates that the structures can survive with damage beyond repair under the high suite. The SATMD(8+4) system proves to be more effective than any other type of TMD system in terms of structural damage indices and this effectiveness becomes more pronounced for the lower hazard suites.

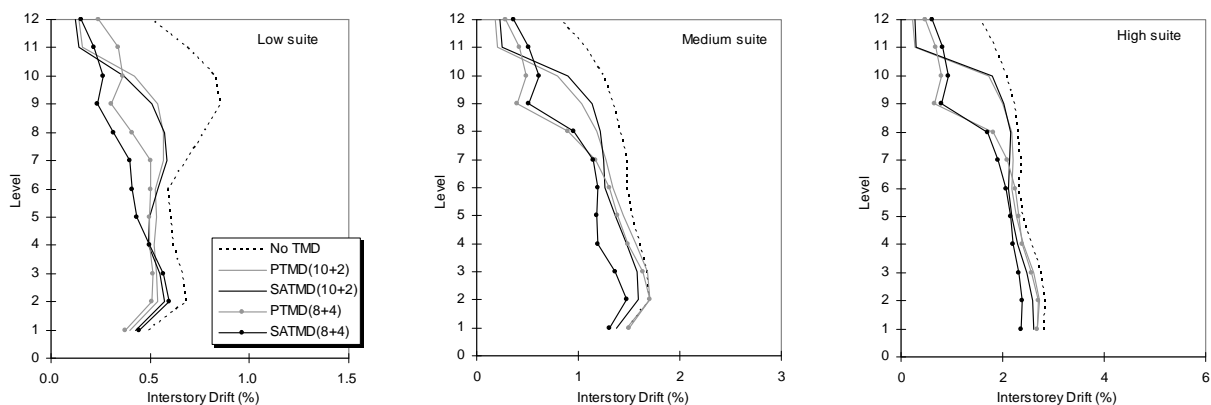


Fig. 7. Interstorey drift ratio (50th Percentile / Low, Medium and High suites)

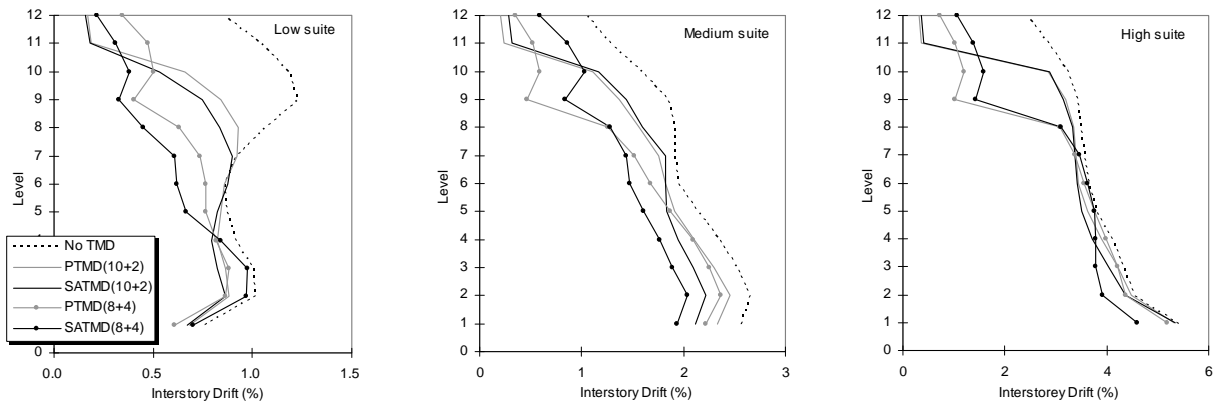


Fig. 8. Interstorey drift ratio (84th Percentile / Low, Medium and High suites)

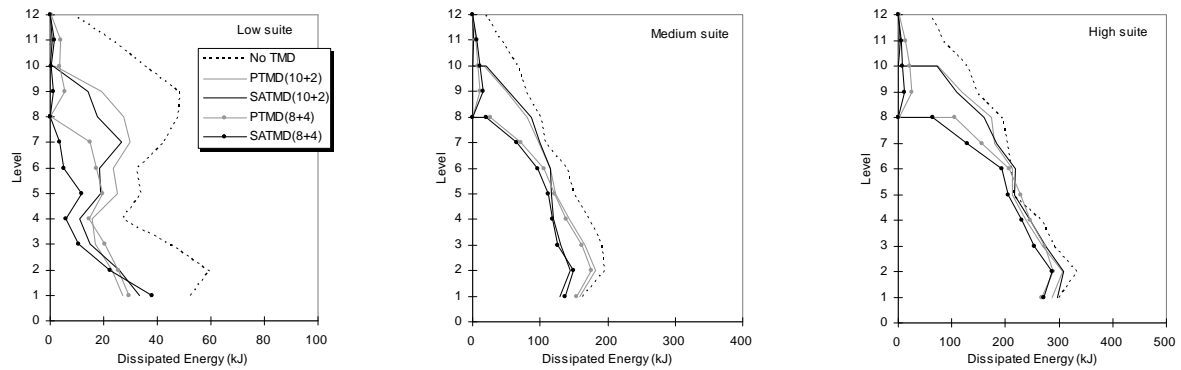


Fig. 9. Story dissipated energy (50th Percentile / Low, Medium and High suites)

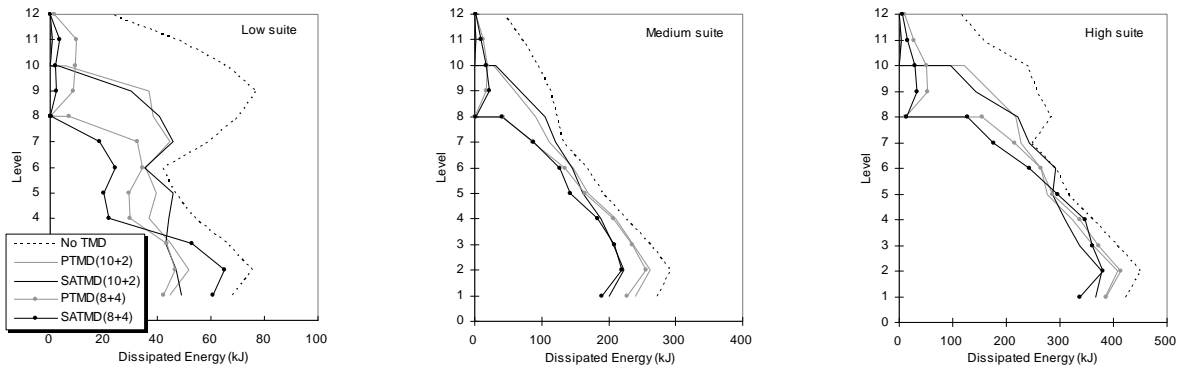


Fig. 10. Story dissipated energy (84th Percentile / Low, Medium and High suites)

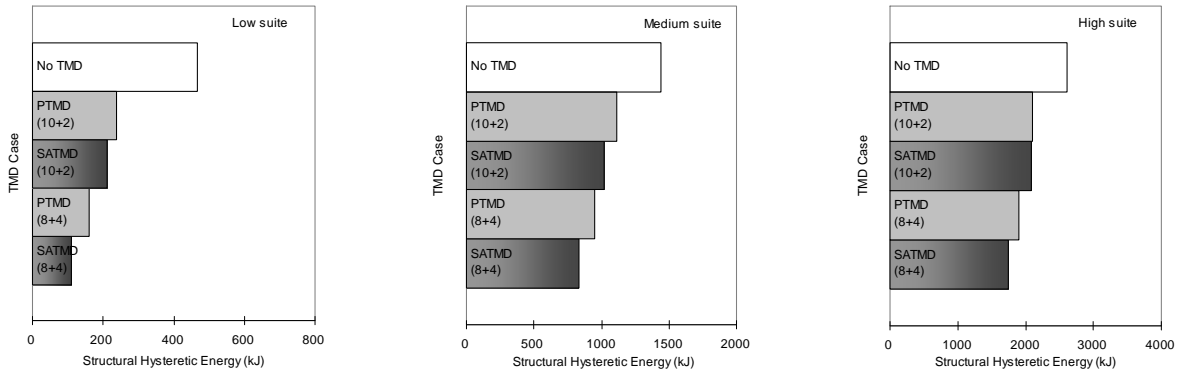


Fig. 11. Structural dissipated energy (50th Percentile / Low, Medium and High suites)

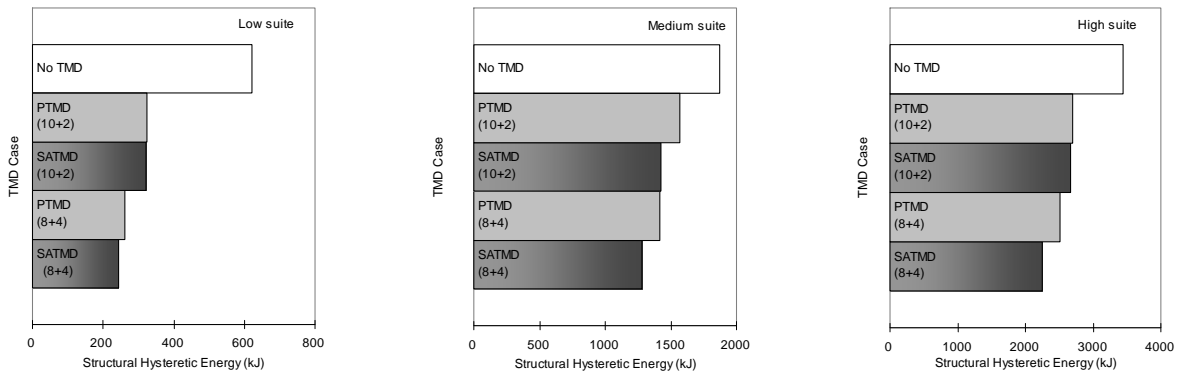


Fig. 12. Structural dissipated energy (84th Percentile / Low, Medium and High suites)

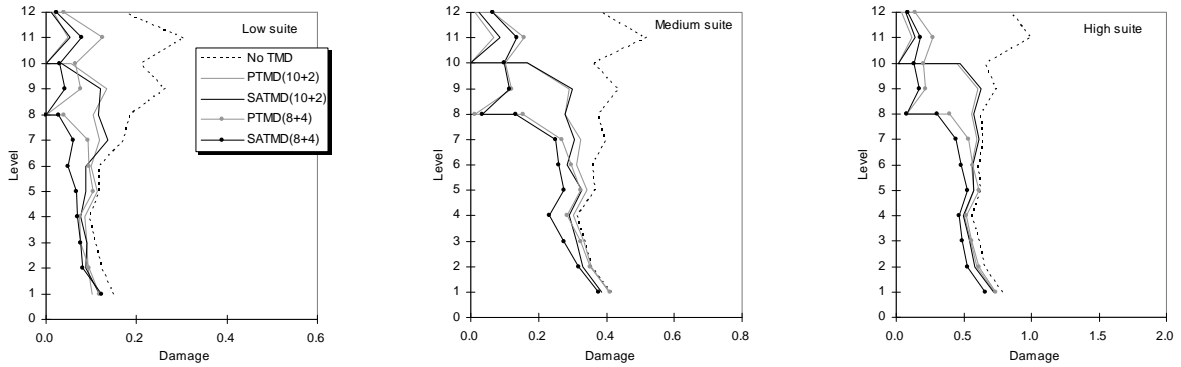


Fig. 13. Story damage (50th Percentile / Low, Medium and High suites)

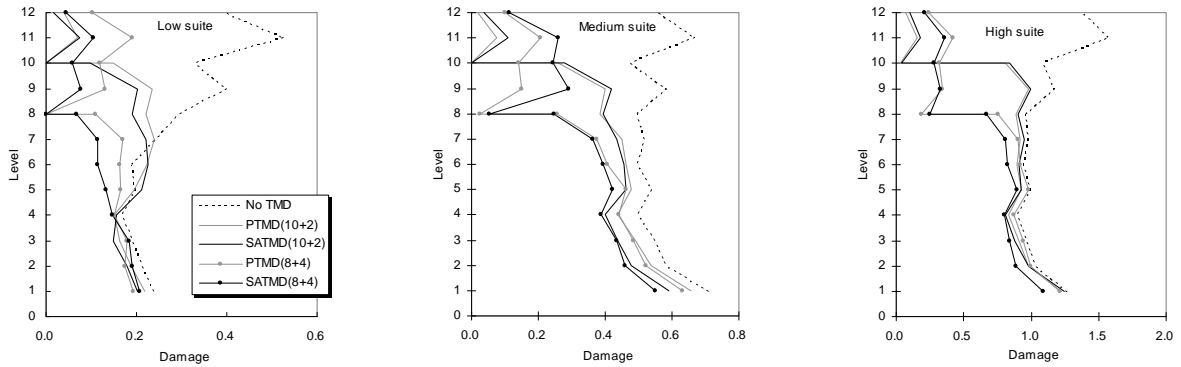
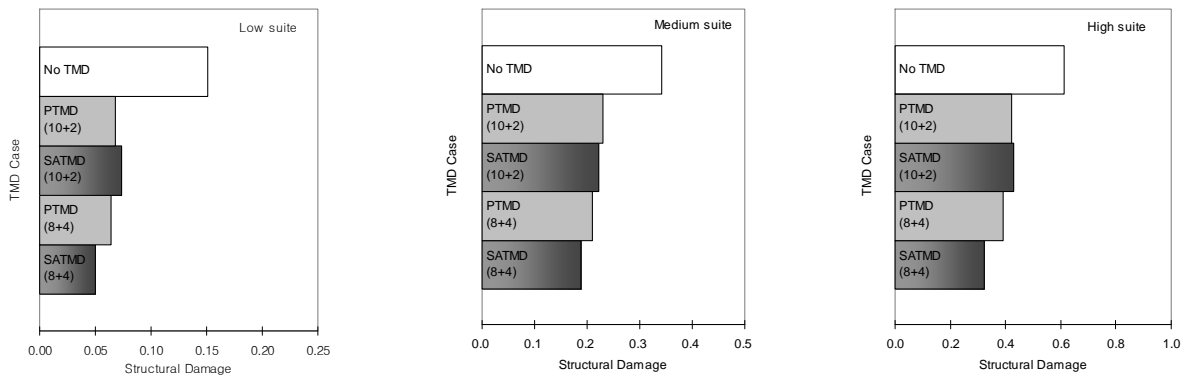
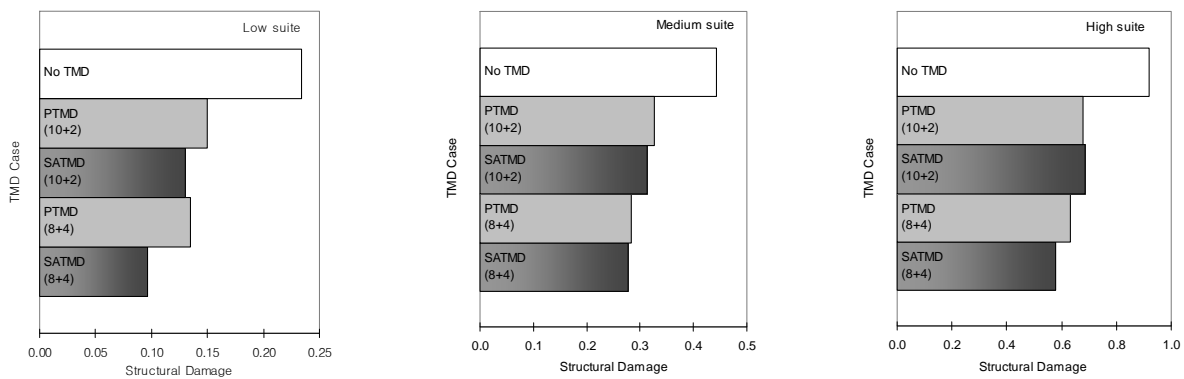


Fig. 14. Story damage (84th Percentile / Low, Medium and High suites)**Fig. 15.** Structural damage (50th Percentile / Low, Medium and High suites)**Fig. 16.** Structural damage (84th Percentile / Low, Medium and High suites)

IX. Conclusions

This paper has investigated the seismic performance of five different nonlinear TMD building systems (No TMD, PTMD (10+2 and 8+4) and SATMD (10+2 and 8+4)) over three probabilistically scaled suites of earthquake records. The seismic demands were based on several assumptions concerning structural parameters and modeling, including P-delta effects, and modified Takeda hysteresis. Performance comparisons were based on statistically calculated interstory drift ratio, hysteretic dissipated energy and practical damage assessments to provide information regarding the cumulative damage to the structure, which may be more important in evaluating potential damage and degradation. The TMD building systems were successful in reducing the seismic demands in statistical point of view for the new designs (10+2 and 8+4).

Overall, the SATMD system provided more robust response mitigation over a range of ground motions within each suite. It should be noted that the PTMD results are optimal, but not necessarily practical. Specifically, the 60-80% damping ratio might not be really achieved. Thus, similar SATMD results indicate that optimal level solutions can be obtained without resulting to infeasibly large non-linear viscous dampers – a significant result. Thus, it might be concluded that the SATMD is the better choice for the seismic case where future input motions are unknown, because it can match potentially infeasible passive solutions with realistic devices, indicating more effective and larger energy dissipation than passive systems.

This research has demonstrated the validity of the realistic SATMD building systems for consideration in future design and construction. The details and results of a set of comparative studies are used to assess the feasibility and effectiveness of such isolation systems. In view of these findings, and the fact that they might be relatively easy to construct using these emerging SA devices, it is concluded that the proposed SATMD building system has the potential to become a practical and effective way to reduce earthquake damage. Thus, these

systems merit further studies to examine their advantages and to further develop experimental validation and design solutions, leading eventually to practical initial designs.

X. References

1. Abdel-Rohman, M.; "Optimal design of active TMD for buildings control"; *Building and Environment*, 19(3); 191-195; 1984.
2. Abe, M.; "Semi-active tuned mass dampers for seismic protection of civil structures"; *Earthquake Engineering & Structural Dynamics*; 25(7), 743-749; 1996.
3. Bertero, V. V., and Uang, C. M.; "Issues and future directions in the use of an energy approach for the seismic-resistant of design structures"; *Nonlinear Seismic Analysis and Design of Reinforced Concrete Buildings*, H. Fajfar P. and Krawinkler, ed., Elsevier Applied Science, Amsterdam; 3-22; 1992.
4. Breneman, S. E.; "Design of Active Control Systems for Multi-Level seismic Resistance"; PhD Thesis, Stanford University; 2000.
5. Chang, C. C., and Yang, H. T. Y.; "Control of buildings using active tuned mass dampers"; *Journal of Engineering Mechanics*; 121(3), 355-366; 1995.
6. Chang, J. C. H., and Soong, T. T.; "Structural control using active tuned mass dampers"; 106(6), 1091-1098; 1980.
7. Charng, P.-H.; "Base isolation for multistorey building structures"; PhD Thesis, University of Canterbury, Christchurch; 1998.
8. Chase, J. G., Mulligan, K. J., Gue, A., Alnot, T., Rodgers, G., Mander, J. B., Elliott, R., Deam, B., Cleeve, L., and Heaton, D.; "Re-shaping hysteretic behaviour using semi-active resettable device dampers"; *Engineering Structures*; 28(10), 1418-1429; 2006.
9. Chey, M. H., Chase, J. G., Mander, J. B., and Carr, A. J.' "Design of semi-active tuned mass damper building systems using resettable devices" 8th Pacific Conference on Earthquake Engineering; Singapore, Paper No. 066; 2007.
10. Conte, J. P., Pister, K. S., and Mahin, S. A.; "Influence of the earthquake ground motion process and structural properties on response characteristics of simple structures"; UBC-EERC Report 90/90, Earthquake Engineering Research Center, Berkeley; 1990.
11. Hrovat, D., Barak, P., and Rabins, M.; "Semi-active versus passive or active tuned mass damper for structural control"; *Journal of Engineering Mechanics Division, ASCE*; 109, 691-705; 1983.
12. Hunt, S. J.; "Semi-active smart-dampers and resettable actuators for multi-level seismic hazard mitigation of steel moment resisting frames"; ME Thesis, University of Canterbury, Christchurch, New Zealand; 2002.
13. Jabbari, F., and Bobrow, J. E.; "Vibration suppression with resettable device"; *Journal of Engineering Mechanics*; 128(9), 916-924; 2002.
14. Jagadish, K. S., Prasad, B. K. R., and Rao, P. V.; "Inelastic vibration absorber subjected to earthquake ground motions"; 7(4), 317-326; 1979.
15. Jury, R. D.; "Seismic load demands on columns of reinforced concrete multistorey frames"; Master Thesis, University of Canterbury, Christchurch, New Zealand; 1978.
16. Kawabata, S., Ohkuma, T., Kanda, J., Kitamura, H., and Ohtake, K.; "Chiba Port Tower. Full-scale measurement of wind actions Part 2. Basic properties of fluctuating wind pressures"; *Journal of Wind Engineering and Industrial Aerodynamics*; 33(1-2), 253-262; 1990.
17. Khan, F. R.; "100 Storey John Hancock Center, Chicago: A case study of the design process"; *Engineering Structures*; 5(1), 10-14; 1983.
18. Kwok, K. C. S., and Macdonald, P. A.; "Full-scale measurements of wind-induced acceleration response of Sydney tower"; *Engineering Structures*; 12(3), 153; 1990.
19. Li, C., Liu, Y., and Wang, Z.; "Active multiple tuned mass dampers: A new control strategy"; *Journal of Structural Engineering*; 129(7), 972-977; 2003.
20. Limpert, E., Stahel, W. A., and Abbt, M.; "Log-normal distributions across the sciences: Keys and clues"; *Bioscience*; 51(5), 341-352; 2001.
21. McNamara, R. J.; "Tuned mass dampers for buildings"; 103(9), 1785-1798; 1977.
22. Miyama, T.; "Seismic response of multi-story frames equipped with energy absorbing story on its top"; 10th World Conference of Earthquake Engineering; 4201-4206; 1992.
23. Mulligan, K., Chase, JG, Mander, JB, Fougere, M, Deam, BL, Danton, G and Elliott, RB.; "Hybrid experimental analysis of semi-active rocking wall systems"; Proc New Zealand Society of Earthquake Engineering Conference (NZSEE), Napier, New Zealand; 2006.
24. Mulligan, K., Miguelgorry, M., Novello, V., Chase, J., Mander, J., Rodgers, G., Carr, A., Deam, B., and Horn, B.; "Semi-active Tuned Mass Damper Systems"; 19th Australasian Conference on Mechanics of Structures and Materials (ACMSM), Christchurch, New Zealand; 2007.

25. Mulligan, K. J.; "Experimental and Analytical Studies of Semi-Active and Passive Structural Control of Buildings"; PhD Thesis, University of Canterbury, Christchurch, New Zealand; 2007.
26. Murakami, K., Kitamura, H., Ozaki, H., and Teramoto, T.; "Design and analysis of a building with the middle-story isolation structural system"; 12th World Conference of Earthquake Engineering, 0857, 1-8; 2000.
27. NZS4203; "New Zealand Standard; Code of Practice for General Structural Design and Design Loadings for Buildings"; Standards Association of New Zealand (SANZ); 1976.
28. NZS4203; "New Zealand Standard; Code of Practice for General Structural Design and Design Loadings for Buildings"; Standards Association of New Zealand (SANZ); 1992.
29. Pan, T.-C., Ling, S.-F., and Cui, W.; "Seismic response of segmental buildings"; Earthquake Engineering & Structural Dynamics; 24(7), 1039-1048; 1995.
30. Pan, T. C., and Cui, W.; "Response of segmental buildings to random seismic motions"; ISET Journal of Engineering Technology; 35(4), 105-112; 1998.
31. Park, Y.-J., and Ang, A. H. S.; "Mechanistic seismic damage model for reinforced concrete"; Journal of Structural Engineering; 111(4), 722-739; 1985.
32. Pinkaew, T., and Fujino, Y.; "Effectiveness of semi-active tuned mass dampers under harmonic excitation"; Engineering Structures; 23(7), 850-856; 2001.
33. Sadek, F., Mohraz, B., Taylor, A. W., and Chung, R. M.; "A method of estimating the parameters of tuned mass dampers for seismic applications"; Earthquake Engineering & Structural Dynamics; 26(6), 617-635; 1997.
34. Sommerville, P., Smith, N., Punyamurthula, S., and Sun, J.; "Development of ground motion time histories for Phase II of the FEMA/SAC steel project"; 1997.
35. Ueda, T., Nakagaki, R., and Koshida, K.; "Suppression of Wind-Induced Vibration of Tower-Shaped Structures by Dynamic Dampers"; Structural Engineering International; 3, 50-53; 1993.
36. Varadarajan, N., and Nagarajaiah, S.; "Wind response control of building with variable stiffness tuned mass damper using empirical mode decomposition/Hilbert transform"; Journal of Engineering Mechanics; 130(4), 451-458; 2004.
37. Villaverde, R.; "Aseismic roof isolation system: Feasibility study with 13-story building"; Journal of Structural Engineering; 128(2), 188-196; 2002.